

# 広島大学学術情報リポジトリ

## Hiroshima University Institutional Repository

Title	UV and IR Spectroscopy of Cold H <sub>2</sub> O <sup>+</sup> -Benzo-Crown Ether Complexes
Author(s)	Inokuchi, Yoshiya; Ebata, Takayuki; Rizzo, Thomas R.
Citation	Journal of Physical Chemistry A , 119 (45) : 11113 - 11118
Issue Date	2015-11-12
DOI	<a href="https://doi.org/10.1021/acs.jpca.5b07033">10.1021/acs.jpca.5b07033</a>
Self DOI	
URL	<a href="https://ir.lib.hiroshima-u.ac.jp/00046472">https://ir.lib.hiroshima-u.ac.jp/00046472</a>
Right	Copyright (c) 2015 American Chemical Society This document is the Accepted Manuscript version of a Published Work that appeared in final form in Journal of Physical Chemistry A, copyright c American Chemical Society after peer review and technical editing by the publisher. To access the final edited and published work see <a href="https://doi.org/10.1021/acs.jpca.5b07033">10.1021/acs.jpca.5b07033</a> .
Relation	



# UV and IR Spectroscopy of Cold $\text{H}_2\text{O}^+$ –Benzo-Crown Ether Complexes

Yoshiya Inokuchi,<sup>‡,\*</sup> Takayuki Ebata,<sup>‡</sup> and Thomas R. Rizzo<sup>†</sup>

*Department of Chemistry, Graduate School of Science, Hiroshima University,  
Higashi-Hiroshima, Hiroshima 739-8526, Japan and Laboratoire de Chimie Physique  
Moléculaire, École Polytechnique Fédérale de Lausanne, Lausanne CH-1015,  
Switzerland*

E-mail: y-inokuchi@hiroshima-u.ac.jp

## Abstract

The  $\text{H}_2\text{O}^+$  radical ion, produced in an electrospray ion source *via* charge transfer from  $\text{Eu}^{3+}$ , is encapsulated in benzo-15-crown-5 (B15C5) or benzo-18-crown-6 (B18C6). We measure UV photodissociation (UVPD) spectra of the  $(\text{H}_2\text{O}\cdot\text{B15C5})^+$  and  $(\text{H}_2\text{O}\cdot\text{B18C6})^+$  complexes in a cold, 22-pole ion trap. These complexes show sharp vibronic bands in the 35700–37600  $\text{cm}^{-1}$  region, similar to the case of neutral B15C5 or B18C6. These results indicate that the positive charge in the complexes is localized on  $\text{H}_2\text{O}$ , giving the forms  $\text{H}_2\text{O}^+\cdot\text{B15C5}$  and  $\text{H}_2\text{O}^+\cdot\text{B18C6}$ , in spite of the fact that the ionization energy of B15C5 and B18C6 is lower than that of  $\text{H}_2\text{O}$ . The formation of the  $\text{H}_2\text{O}^+$  complexes and the suppression of the  $\text{H}_3\text{O}^+$  production through the reaction of  $\text{H}_2\text{O}^+$  and  $\text{H}_2\text{O}$  can be attributed to the encapsulation of hydrated  $\text{Eu}^{3+}$  clusters by B15C5 and B18C6. On the other hand, the main fragment ions subsequent to the UV excitation of these complexes are  $\text{B15C5}^+$  and  $\text{B18C6}^+$  radical ions; the

charge transfer occurs from  $\text{H}_2\text{O}^+$  to B15C5 and B18C6 after the UV excitation. The position of the band origin for the  $\text{H}_2\text{O}^+\cdot\text{B18C6}$  complex ( $36323\text{ cm}^{-1}$ ) is almost the same as that for  $\text{Rb}^+\cdot\text{B18C6}$  ( $36315\text{ cm}^{-1}$ ); the strength of the intermolecular interaction of  $\text{H}_2\text{O}^+$  with B18C6 is similar to that of  $\text{Rb}^+$ . The spectral features of the  $\text{H}_2\text{O}^+\cdot\text{B15C5}$  complex also resemble those of the  $\text{Rb}^+\cdot\text{B15C5}$  ion. We measure IR-UV spectra of these complexes in the CH and OH stretching region. Four conformers are found for the  $\text{H}_2\text{O}^+\cdot\text{B15C5}$  complex, but there is one dominant form for the  $\text{H}_2\text{O}^+\cdot\text{B18C6}$  ion. This study demonstrates the production of radical ions by charge transfer from multivalent metal ions, their encapsulation by host molecules, and separate detection of their conformers by cold UV spectroscopy in the gas phase.

Keywords: lanthanide, europium, 18-crown-6, 15-crown-5, encapsulation, water, crown ether, infrared, ion trap, electrospray, solvent effect

\*To whom correspondence should be addressed.

‡Hiroshima University

†École Polytechnique Fédérale de Lausanne

## 1. Introduction

One of the advantages of electrospray in mass spectrometry is its ability to introduce ions from solution directly into vacuum without destroying them, even if molecules are large and non-volatile.<sup>1-2</sup> However, the electrospray process sometimes occurs under harsh conditions due to high electric fields, inducing a number of chemical reactions. In addition, the reduction of the positive charge from multiply charged metal ions often occurs in electrospray, which is due to their higher ionization energy (IE) than that of solvent molecules.<sup>3</sup> In our experimental efforts to produce host-guest complexes of metal ions by electrospray, we found that when using solutions of lanthanide salts and host molecules, radical ions of solvent are efficiently produced and encapsulated in the host cavities. In this study, we report the production of the  $\text{H}_2\text{O}^+$  radical ion and its encapsulation in the cavity of benzo-15-crown-5 (B15C5) or benzo-18-crown-6 (B18C6) using electrospray, forming  $(\text{H}_2\text{O}\cdot\text{B15C5})^+$  and  $(\text{H}_2\text{O}\cdot\text{B18C6})^+$  complexes. In order to examine the electronic and geometric structures of these complexes, we perform UV photodissociation (UVPD) and IR-UV double-resonance spectroscopy in a cold, 22-pole ion trap.<sup>4</sup> On the basis of the spectroscopic results, we can determine the structure of these complexes and investigate charge transfer (CT) processes that occur within them.

## 2. Experimental Method

The experiment is performed with a tandem mass spectrometer equipped with a nanoelectrospray ion source.<sup>4-6</sup> We inject a solution of  $\text{EuCl}_3\cdot 6\text{H}_2\text{O}$  and B15C5 or B18C6 ( $\sim 200 \mu\text{M}$  each) in methanol/water ( $\sim 98:2$  volume ratio) *via* the nanoelectrospray source. While  $(\text{H}_2\text{O}\cdot\text{B15C5})^+$  and  $(\text{H}_2\text{O}\cdot\text{B18C6})^+$  complexes are produced in this source, we cannot find bare  $\text{Eu}^{3+}$  ion or complexes containing it.

Mass spectra of the  $\text{EuCl}_3 \cdot 6\text{H}_2\text{O}$  solutions with B15C5 and B18C6 are displayed in Fig. 1S of the Supporting Information. These spectra clearly show that the  $(\text{H}_2\text{O} \cdot \text{B15C5})^+$  and  $(\text{H}_2\text{O} \cdot \text{B18C6})^+$  complexes are formed, and that the  $\text{H}_3\text{O}^+ \cdot \text{B15C5}$  or  $\text{H}_3\text{O}^+ \cdot \text{B18C6}$  complex is not seen in this experiment. The signals  $m/Z = \sim 1.0$  above the  $(\text{H}_2\text{O} \cdot \text{B15C5})^+$  and  $(\text{H}_2\text{O} \cdot \text{B18C6})^+$  complexes ( $m/Z = 287$  for B15C5 and 331 for B18C6) can be assigned to the complexes having one  $^{13}\text{C}$  atom. The parent ions of interest are selected in a quadrupole mass filter and injected into a 22-pole RF ion trap, which is cooled by a closed-cycle He refrigerator to 6 K. The trapped ions are cooled internally and translationally to  $\sim 10$  K through collisions with cold He buffer gas,<sup>4,5,7-8</sup> which is synchronously injected into the trap. The trapped ions are then irradiated with a tunable UV laser pulse, which causes some fraction of them to dissociate. The resulting charged photofragments, as well as the remaining parent ions, are released from the trap, analyzed by a second quadrupole mass filter, and detected with a channeltron electron multiplier. The UVPD spectra of parent ions are obtained by plotting the yield of a particular photofragment ion as a function of the wavenumber of the UV laser. We also measure conformer-specific infrared spectra using IR-UV double-resonance spectroscopy. In these experiments, the output pulse of an IR OPO precedes the UV pulse by  $\sim 100$  ns and counter-propagates collinearly with it through the ion trap. Absorption of the IR light by the ions in a specific conformer induces the depopulation of the ground state, resulting in the reduction of the net UV absorption of this conformer.<sup>9</sup> The wavenumber of the UV laser is then fixed to a vibronic transition of this conformer for monitoring the conformer-selective IR-induced depletion of the UVPD yield, and the wavenumber of the OPO is scanned in the light-atom stretching region ( $2600\text{--}3800\text{ cm}^{-1}$ ) while monitoring the number of fragment ions. IR-UV

depletion spectra are obtained by plotting the yield of a particular photofragment as a function of the OPO wavenumber.

### 3. Results and Discussion

#### 3.1 (H<sub>2</sub>O•B18C6)<sup>+</sup> complex

Figures 1a and 1b display the UVPD spectra of the (H<sub>2</sub>O•B18C6)<sup>+</sup> and Rb<sup>+</sup>•B18C6 complexes, respectively; the latter spectrum was reported in our previous study.<sup>10</sup> The spectrum of the (H<sub>2</sub>O•B18C6)<sup>+</sup> complex is measured by monitoring the yield of B18C6<sup>+</sup> photofragment. Neutral B18C6 exhibits band origins at 35167 cm<sup>-1</sup> and around 35650 cm<sup>-1</sup> for four conformers.<sup>11</sup> Hence, the vibronic bands in the spectrum of the (H<sub>2</sub>O•B18C6)<sup>+</sup> complex can be assigned to the absorption of the B18C6 component. This suggests that B18C6 in the (H<sub>2</sub>O•B18C6)<sup>+</sup> complex remains neutral, and the complex has the structure H<sub>2</sub>O<sup>+</sup>•B18C6. In the case of alkali metal ion–B18C6 complexes, M<sup>+</sup>•B18C6, the position of the band origin reflects the strength of the intermolecular interaction between M<sup>+</sup> and B18C6; being located at 36398, 36315, and 36234 cm<sup>-1</sup> for the K<sup>+</sup>, Rb<sup>+</sup>, and Cs<sup>+</sup> complexes, respectively.<sup>10</sup> As shown in Fig. 1a, the H<sub>2</sub>O<sup>+</sup>•B18C6 complex has its band origin at 36323 cm<sup>-1</sup>, closest to that of the Rb<sup>+</sup>•B18C6 complex (36315 cm<sup>-1</sup>). In addition, the vibronic structure is quite similar between the spectra of H<sub>2</sub>O<sup>+</sup>•B18C6 and Rb<sup>+</sup>•B18C6. This suggests that the strength of intermolecular interaction of H<sub>2</sub>O<sup>+</sup> with B18C6 is comparable to that of Rb<sup>+</sup>.

In order to determine the structure and examine the coexistence of multiple conformers, we measure IR spectra of the H<sub>2</sub>O<sup>+</sup>•B18C6 complex by IR-UV double-resonance spectroscopy. Figure 2a shows the IR-UV spectrum of the H<sub>2</sub>O<sup>+</sup>•B18C6 complex along with that of the Rb<sup>+</sup>•B18C6 ion (Fig. 2b) from our previous

study.<sup>10</sup> These spectra are obtained by fixing the UV frequency at the respective band origins (36323 and 36315  $\text{cm}^{-1}$ ). In the case of  $\text{H}_2\text{O}^+\cdot\text{B18C6}$ , the frequency of the IR OPO was scanned up to  $\sim 3700 \text{ cm}^{-1}$ , but no band was observed in the 3200–3700  $\text{cm}^{-1}$  region (see Fig. 2S of the Supporting Information). For the  $\text{Rb}^+\cdot\text{B18C6}$  complex, all the strong vibronic bands in the UVPD spectrum (Fig. 1b) show the same IR-UV spectrum as that in Fig. 2b.<sup>10</sup> Similarly, all the IR-UV spectra of the  $\text{H}_2\text{O}^+\cdot\text{B18C6}$  complex are identical for the strong vibronic bands in Fig. 1a, indicating that there is only one dominant conformer. Weak vibronic bands in the 36150–36300  $\text{cm}^{-1}$  region of Fig. 1a are attributed to a minor conformer because of their different vibronic structure from that of the main conformer from 36323  $\text{cm}^{-1}$ . In the IR-UV spectrum of the  $\text{Rb}^+\cdot\text{B18C6}$  ion (Fig. 2b), absorption of the CH stretching vibrations is observed mainly around 2900  $\text{cm}^{-1}$ . The IR spectrum of the  $\text{H}_2\text{O}^+\cdot\text{B18C6}$  complex measured at 36323  $\text{cm}^{-1}$  shows strong absorption in the 3000–3200  $\text{cm}^{-1}$  region in addition to weaker bands due to the CH stretches at  $\sim 2900 \text{ cm}^{-1}$ . Hence, the strong bands at 3026 and 3051  $\text{cm}^{-1}$  can be assigned to the OH stretching vibrations of the  $\text{H}_2\text{O}^+$  component. The frequency of the symmetric ( $\nu_1$ ) and asymmetric ( $\nu_3$ ) OH stretching vibrations of  $\text{H}_2\text{O}^+$  in the gas phase was reported to be 3212.86 and 3259.04  $\text{cm}^{-1}$ , respectively.<sup>12</sup> It is thus likely that the OH groups of the  $\text{H}_2\text{O}^+$  component in the  $\text{H}_2\text{O}^+\cdot\text{B18C6}$  complex form hydrogen bonds with the B18C6 part.

We then examined theoretically the possibility that the complex in this study was not the  $\text{H}_2\text{O}^+$  cluster but the  $\text{H}_3\text{O}^+$  one. We performed the conformational search, geometry optimization, and calculations of electronic transitions for the  $\text{H}_3\text{O}^+\cdot\text{B18C6}$  complex; the details of the calculations were explained in the Supporting Information. As mentioned above, the position of the band origin reflects the strength of the

intermolecular interaction between cations and B18C6, and calculated transition energies by time-dependent density functional theory (TD-DFT) reproduce the observed ones in the UVPD spectra very well, with an accuracy of  $\sim 20 \text{ cm}^{-1}$ .<sup>10</sup> As seen in Fig. 3S of the Supporting Information, the most stable form of the  $\text{H}_3\text{O}^+\cdot\text{B18C6}$  complex is predicted to have the transition to the first excited state at  $36736 \text{ cm}^{-1}$ , much higher than that observed in Fig. 1a ( $36323 \text{ cm}^{-1}$ ). Hence, it is probable that the complex formed in this experiment is surely the  $\text{H}_2\text{O}^+\cdot\text{B18C6}$  ion.

### 3.2 ( $\text{H}_2\text{O}\cdot\text{B15C5}$ )<sup>+</sup> complex

Figure 3a shows the UVPD spectrum of the ( $\text{H}_2\text{O}\cdot\text{B15C5}$ )<sup>+</sup> complex. The band origin of neutral B15C5 is found at  $35645$ ,  $35653$ , and  $36217 \text{ cm}^{-1}$  for three conformers.<sup>13</sup> The vibronic bands of the ( $\text{H}_2\text{O}\cdot\text{B15C5}$ )<sup>+</sup> complex in Fig. 3a are thus assignable to the absorption of the B15C5 part; the  $\text{H}_2\text{O}$  part mainly carries the positive charge in this complex, giving a structure of the form  $\text{H}_2\text{O}^+\cdot\text{B15C5}$ . As mentioned above, the  $\text{H}_2\text{O}^+$  radical ion interacts with the B18C6 component similarly to the  $\text{Rb}^+$  ion. Figure 3b displays the UVPD spectrum of the  $\text{Rb}^+\cdot\text{B15C5}$  complex.<sup>10</sup> The vibronic bands of the  $\text{Rb}^+\cdot\text{B15C5}$  complex are attributed to three isomers (Rb-I, Rb-II, and Rb-III).<sup>10</sup>

We apply IR-UV spectroscopy to the  $\text{H}_2\text{O}^+\cdot\text{B15C5}$  complex in the CH and OH stretching regions. Figure 4 shows the IR-UV spectra of the  $\text{H}_2\text{O}^+\cdot\text{B15C5}$  ion with those of conformers Rb-II and Rb-III of  $\text{Rb}^+\cdot\text{B15C5}$ .<sup>10</sup> The IR-UV spectra of the  $\text{H}_2\text{O}^+\cdot\text{B15C5}$  complex are measured by monitoring the photofragment yield at the UV positions (1–4) highlighted by arrows in Fig. 3a. The four IR-UV spectra of the  $\text{H}_2\text{O}^+\cdot\text{B15C5}$  complex show different spectral features. Hence, there are at least four isomers for the  $\text{H}_2\text{O}^+\cdot\text{B15C5}$  complex in our experiment. In contrast to the case of the

$\text{H}_2\text{O}^+\cdot\text{B18C6}$  complex described above, it is not possible to identify clearly the OH stretching bands of the  $\text{H}_2\text{O}^+$  component in these congested IR spectra. However, since the  $\text{Rb}^+$  complex has strong CH stretching bands only in the 2870–2990  $\text{cm}^{-1}$  region (Figs. 4e and 4f),<sup>10</sup> the strong bands below 2800  $\text{cm}^{-1}$  in the IR spectra of the  $\text{H}_2\text{O}^+$  complex can tentatively be assigned to the OH stretching vibration(s).

Zwier and coworkers and our group have reported that the vibronic structure of B15C5 around the band origin is a good diagnosis of the conformation around the phenyl ring; conformers in which the  $\beta$  carbon atoms (C4 and C14 atoms, see Scheme 1 of Ref. 10) are displaced largely from the plane of the phenyl ring show intense Franck-Condon progressions.<sup>10, 13-14</sup> The vibronic structure of the  $\text{H}_2\text{O}^+\cdot\text{B15C5}$  complex is quite similar to that of the  $\text{Rb}^+\cdot\text{B15C5}$  ion in the 36300–36900  $\text{cm}^{-1}$  region, which corresponds to Rb-II and Rb-III. In the isomers that show Rb-II and Rb-III (isomers Rb-A and Rb-B, see Figs. 7 and 8 of Ref. 10), the  $\beta$  carbon atoms are located largely out of the benzene plane. This suggests that isomers 3 and 4 of  $\text{H}_2\text{O}^+\cdot\text{B15C5}$  have the  $\beta$  carbon atoms displaced largely from the phenyl plane, similar to Rb-A and Rb-B of  $\text{Rb}^+\cdot\text{B15C5}$ . In contrast, isomers 1 and 2 of  $\text{H}_2\text{O}^+\cdot\text{B15C5}$  show strong origin bands, and their progressions are not so extensive. This suggests that the  $\beta$  carbon atoms of isomers 1 and 2 are located almost in the benzene plane.

We performed the conformational search, geometry optimization, and calculations of electronic transitions also for the  $\text{H}_3\text{O}^+\cdot\text{B15C5}$  complex. The calculated results are shown in Fig. 4S of the Supporting Information. The electronic transition energy of the most stable  $\text{H}_3\text{O}^+\cdot\text{B15C5}$  conformer is estimated as 36969  $\text{cm}^{-1}$ , higher than those of the  $\text{H}_2\text{O}^+\cdot\text{B15C5}$  isomers in the UVPD spectrum (Fig. 3a).

Therefore, the complex examined in this study is not  $\text{H}_3\text{O}^+\cdot\text{B15C5}$  but surely  $\text{H}_2\text{O}^+\cdot\text{B15C5}$ .

### 3.3 Energetics of the $(\text{H}_2\text{O}\cdot\text{B18C6})^+$ and $(\text{H}_2\text{O}\cdot\text{B15C5})^+$ complexes

Figure 5 shows schematic potential energy surfaces proposed for the  $(\text{H}_2\text{O}\cdot\text{B18C6})^+$  complex. The right- and left-hand sides in Fig. 5 represent the dissociation limit to  $(\text{H}_2\text{O} + \text{B18C6}^+)$  and  $(\text{H}_2\text{O}^+ + \text{B18C6})$ , respectively. The energy of these dissociation limits is obtained from the IEs of  $\text{H}_2\text{O}$  (12.65 eV) and benzene (9.24384 eV).<sup>15-16</sup> We performed the geometry optimization of  $(\text{H}_2\text{O}\cdot\text{B18C6})^+$  at the M05-2X/6-31+G(d) level of theory using the GAUSSIAN 09 program package.<sup>17</sup> However, all the optimized structures have the  $\text{H}_2\text{O}\cdot\text{B18C6}^+$  form; the stable structures of the  $(\text{H}_2\text{O}\cdot\text{B18C6})^+$  complex are shown in Fig. 6S of the Supporting Information. Since the UVPD spectra in Fig. 1 demonstrate that the strength of the intermolecular interaction of  $\text{H}_2\text{O}^+$  with B18C6 is almost the same as that of  $\text{Rb}^+$ , the binding energy (BE) between  $\text{H}_2\text{O}^+$  and B18C6 is estimated to be 2.02 eV, which is the calculated value between  $\text{Rb}^+$  and B18C6 in our previous study<sup>10</sup> and close to the experimental value between  $\text{Rb}^+$  and 18-crown-6 (1.98 eV).<sup>18</sup> The band origin of the  $\text{H}_2\text{O}^+\cdot\text{B18C6}$  complex is found at 4.50 eV ( $36323\text{ cm}^{-1}$ ) as shown in Fig. 1a. The BE between  $\text{H}_2\text{O}$  and  $\text{B18C6}^+$  is estimated as 0.58 eV by our quantum chemical calculations described above. The energy of the  $\text{H}_2\text{O}^+\cdot\text{B18C6}$  complex is substantially ( $\sim 1.97$  eV) higher than that of the  $\text{H}_2\text{O}\cdot\text{B18C6}^+$  ion due to higher IE of  $\text{H}_2\text{O}$  than that of B18C6. As shown in Fig. 7S of the Supporting Information, the  $\text{H}_2\text{O}\cdot\text{B18C6}^+$  forms are calculated to have at least one strong OH stretching vibration in the  $3300\text{--}3700\text{ cm}^{-1}$  region, which is not consistent with the measured IR-UV spectrum in Fig. 2S of the Supporting

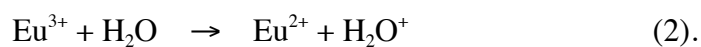
Information. This confirms that the charge sits on the water and the complex that we observe in our experiment exists as  $\text{H}_2\text{O}^+\cdot\text{B18C6}$ .

The main photoproduct of  $\text{H}_2\text{O}^+\cdot\text{B18C6}$  is  $\text{B18C6}^+$ , indicating that the CT occurs from  $\text{H}_2\text{O}^+$  to  $\text{B18C6}$  after the UV excitation,



In the  $\text{H}_2\text{O}^+\cdot\text{B18C6}$  complex, the distribution of the positive charge will be similar to the non-bonding orbital of the  $\text{H}_2\text{O}$  moiety. Therefore, in order for the  $\text{H}_2\text{O}^+\cdot\text{B18C6}$  complex to transfer an electron or the positive charge between  $\text{B18C6}$  and  $\text{H}_2\text{O}^+$ , the non-bonding orbital of  $\text{H}_2\text{O}$  and  $\pi$  orbitals of the benzene ring should be fairly overlapped. Probably the overlap is not necessarily sufficient in the stable form of the  $\text{H}_2\text{O}^+\cdot\text{B18C6}$  complex, providing a long lifetime to this complex. After the UV excitation of the  $\text{H}_2\text{O}^+\cdot\text{B18C6}$  complex, the internal conversion (IC) occurs to the electronic ground state, providing enough internal energy for the structural change to promote the sufficient overlap of the molecular orbitals between  $\text{H}_2\text{O}$  and  $\text{B18C6}$ , leading to the CT from  $\text{H}_2\text{O}^+$  to  $\text{B18C6}$ . Benzene radical cation has a  $(\pi, \pi)$  excited state at  $\sim 2.8$  eV above the electronic ground state.<sup>26-27</sup> Therefore, the electronic state of the fragment  $\text{B18C6}^+$  can be the ground state or the excited  $(\pi, \pi)$  state. Since the IE of  $\text{B15C5}$  is similar to that of  $\text{B18C6}$ , the situation described above for  $\text{H}_2\text{O}^+\cdot\text{B18C6}$  is applicable to  $\text{H}_2\text{O}^+\cdot\text{B15C5}$ . The UV spectra of the  $\text{H}_2\text{O}^+\cdot\text{B18C6}$  and  $\text{H}_2\text{O}^+\cdot\text{B15C5}$  show quite sharp features. The width of the vibronic structures ( $\sim 2.7$   $\text{cm}^{-1}$ ) imply that the lifetime of the excited states is longer than  $\sim 2.0$  ps. However, CT processes usually occur with a timescale shorter than 1 ps.<sup>28</sup> Hence, the first step after the photoexcitation is probably the IC from the first excited state to the ground state, followed by the CT and dissociation.

Another interesting finding in this study is that the positive charge is localized not on the crown ethers but on H<sub>2</sub>O in the (H<sub>2</sub>O•B18C6)<sup>+</sup> and (H<sub>2</sub>O•B15C5)<sup>+</sup> complexes, in spite of the fact that the IE of H<sub>2</sub>O is higher than that of the crown ethers. In addition, our experiment does not show the formation of the H<sub>3</sub>O<sup>+</sup>•B18C6 or H<sub>3</sub>O<sup>+</sup>•B15C5 complex; the H<sub>2</sub>O<sup>+</sup> radical cation undergoes ultrafast proton transfer reactions with neutral H<sub>2</sub>O in neat liquid water and water clusters within a few hundreds of fs, providing H<sub>3</sub>O<sup>+</sup> and OH.<sup>19-24</sup> These results in this study can be attributed to encapsulation effects of B18C6 and B15C5. In the mass spectrum of B15C5 (Fig. 1S(a) of the Supporting Information), Eu<sup>2+</sup>•B15C5 and Eu<sup>2+</sup>•B15C5•H<sub>2</sub>O complexes are also observed with H<sub>2</sub>O<sup>+</sup>•B15C5. This result implies following formation processes of the H<sub>2</sub>O<sup>+</sup> complexes. In solution, the Eu<sup>3+</sup> ion is stabilized by solvation. In the (EuCl<sub>3</sub>•6H<sub>2</sub>O + B15C5) solution, the Eu<sup>3+</sup> ion can be encapsulated inside the B15C5 cavity together with a few H<sub>2</sub>O molecules. This may be possible, because the Eu<sup>3+</sup> ion has an ionic radius (0.95 Å for 6 coordination number) smaller than that of Na<sup>+</sup> (1.02 Å).<sup>25</sup> The H<sub>2</sub>O molecules may be bonded to the Eu<sup>3+</sup> ion separately from each other through Eu<sup>3+</sup>•••OH<sub>2</sub> bonds. In the desolvation process, the Eu<sup>3+</sup> ion undergoes the CT from Eu<sup>3+</sup> to water,<sup>3-4</sup>



The third IE of Eu is 24.92 eV,<sup>25</sup> which is substantially higher than the IE of H<sub>2</sub>O (12.65 eV).<sup>15</sup> When the CT occurs from Eu<sup>3+</sup> to H<sub>2</sub>O inside the cavity, the H<sub>2</sub>O<sup>+</sup> cation does not have a chance to react with other H<sub>2</sub>O molecules to form H<sub>3</sub>O<sup>+</sup>. The Eu<sup>2+</sup> and H<sub>2</sub>O<sup>+</sup> ions produced in the B15C5 cavity separate from each other, providing the H<sub>2</sub>O<sup>+</sup>•B15C5, Eu<sup>2+</sup>•B15C5, and Eu<sup>2+</sup>•B15C5•H<sub>2</sub>O complexes. The mass spectrum of B15C5 shows that the H<sub>2</sub>O<sup>+</sup>•B15C5 complex is much more abundant than Eu<sup>2+</sup>•B15C5 and

$\text{Eu}^{2+}\cdot\text{B15C5}\cdot\text{H}_2\text{O}$  (Fig. 1S(a)). This is probably because the  $\text{H}_2\text{O}^+$  ion has a matching in size with B15C5 much better than  $\text{Eu}^{2+}$  or  $\text{Eu}^{2+}\cdot\text{H}_2\text{O}$ .

#### 4. Summary

In our electrospray ion source, charge transfer from  $\text{Eu}^{3+}$  to water occurs and produces the  $\text{H}_2\text{O}^+$  radical cation in the cavity of B15C5 or B18C6, forming the  $\text{H}_2\text{O}^+\cdot\text{B15C5}$  or  $\text{H}_2\text{O}^+\cdot\text{B18C6}$  complex. We observed the UVPD spectra of the  $\text{H}_2\text{O}^+\cdot\text{B15C5}$  and  $\text{H}_2\text{O}^+\cdot\text{B18C6}$  complexes in a cold, 22-pole ion trap. These complexes show sharp bands in the UV region similar to the  $S_1-S_0$  transition of neutral B15C5 and B18C6, suggesting that the positive charge in the complexes is localized on  $\text{H}_2\text{O}$ . On the other hand, the primary fragment ions subsequent to UV excitation of these complexes are  $\text{B15C5}^+$  and  $\text{B18C6}^+$ , which means that charge transfer occurs from  $\text{H}_2\text{O}^+$  to B15C5 and B18C6 subsequent to UV photoexcitation. The vibronic structure of the  $\text{H}_2\text{O}^+\cdot\text{B18C6}$  complex is quite similar to that of  $\text{Rb}^+\cdot\text{B18C6}$ , implying that the strength of the intermolecular interaction of  $\text{H}_2\text{O}^+$  with B18C6 is comparable to that of  $\text{Rb}^+$ . The UV spectral features of the  $\text{H}_2\text{O}^+\cdot\text{B15C5}$  complex also resemble those of the  $\text{Rb}^+\cdot\text{B15C5}$  ion. We measure IR-UV spectra of these complexes in the CH and OH stretching region; four conformers are identified for the  $\text{H}_2\text{O}^+\cdot\text{B15C5}$  complex, but there is only one for the  $\text{H}_2\text{O}^+\cdot\text{B18C6}$  ion. In this study, we have demonstrated the production of radical cations by charge transfer from multivalent metal ions, their encapsulation by host molecules, and separate detection of their conformers by cold UV spectroscopy in the gas phase.

## Acknowledgment

This work is partly supported by the Swiss National Science foundation through grant 200020\_152804 and École Polytechnique Fédérale de Lausanne (EPFL). YI and TE thank the support from JSPS through the program “Strategic Young Researcher Overseas Visits Program for Accelerating Brain Circulation”.

**Supporting Information Available:** Electrospray mass spectra (Fig. 1S), an IR-UV spectrum of  $\text{H}_2\text{O}^+\cdot\text{B18C6}$  in the 2500–3700  $\text{cm}^{-1}$  region (Fig. 2S), calculated UV spectra of the  $\text{H}_3\text{O}^+\cdot\text{B18C6}$  and  $\text{H}_3\text{O}^+\cdot\text{B15C5}$  complexes (Figs. 3S and 4S), the structure of the most stable conformers for  $\text{H}_3\text{O}^+\cdot\text{B18C6}$  and  $\text{H}_3\text{O}^+\cdot\text{B15C5}$  (Fig. 5S), the optimized structures of the  $(\text{H}_2\text{O}\cdot\text{B18C6})^+$  complex (Fig. 6S), the calculated IR spectra for the  $(\text{H}_2\text{O}\cdot\text{B18C6})^+$  complex (Fig. 7S), and a full list of authors of Ref. 17. This material is available free of charge *via* the internet at <http://pubs.acs.org>.

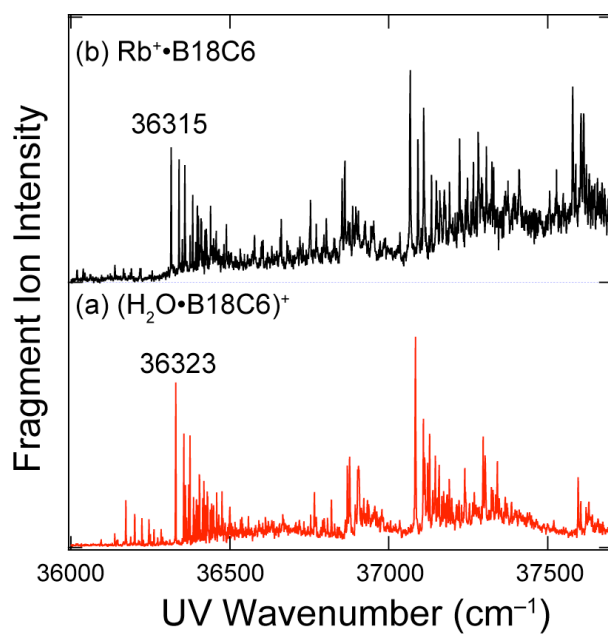


**Figure 1.** The UVPD spectra of the (a) (H<sub>2</sub>O•B18C6)<sup>+</sup> and (b) Rb<sup>+</sup>•B18C6 complexes (Ref. 10).

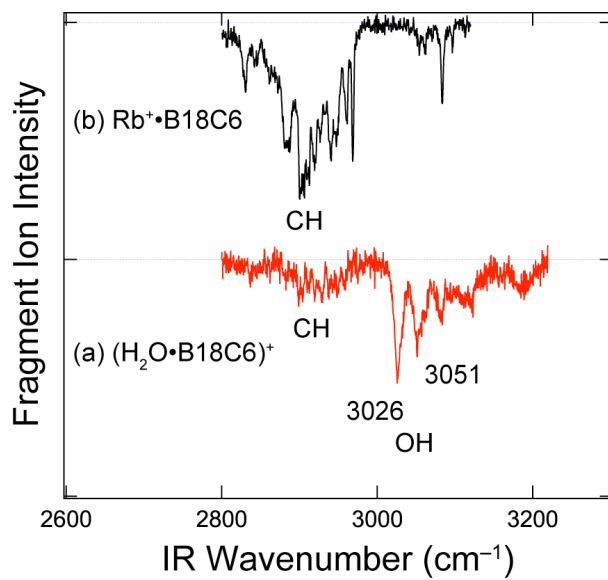


**Figure 2.** The IR-UV spectra of the (a) (H<sub>2</sub>O•B18C6)<sup>+</sup> and (b) Rb<sup>+</sup>•B18C6 complexes (Ref. 10).

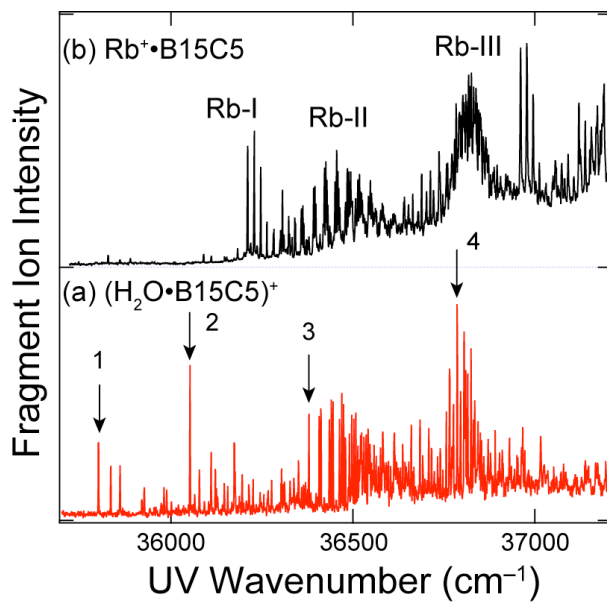


**Figure 3.** (a) The UVPD spectrum of the  $(\text{H}_2\text{O}\cdot\text{B15C5})^+$  complex. (b) The UVPD spectrum of the  $\text{Rb}^+\cdot\text{B15C5}$  complex (Ref. 10). Arrows indicate the position where the IR-UV spectra are measured for the  $(\text{H}_2\text{O}\cdot\text{B15C5})^+$  complex.

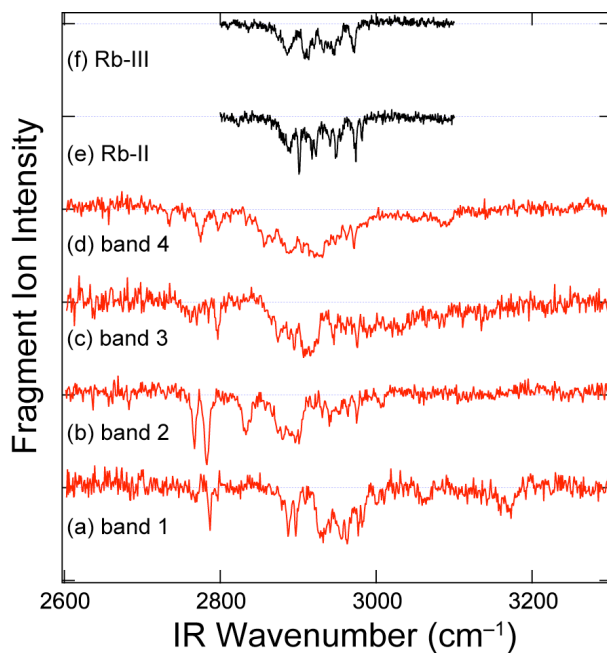


**Figure 4.** The IR-UV spectra of the (a–d)  $(\text{H}_2\text{O}\cdot\text{B15C5})^+$  and (e, f)  $\text{Rb}^+\cdot\text{B15C5}$  complexes (Ref. 10). The numbers 1–4 indicate the UV position where these IR-UV spectra are observed for the  $(\text{H}_2\text{O}\cdot\text{B15C5})^+$  complex (see Fig. 3a).

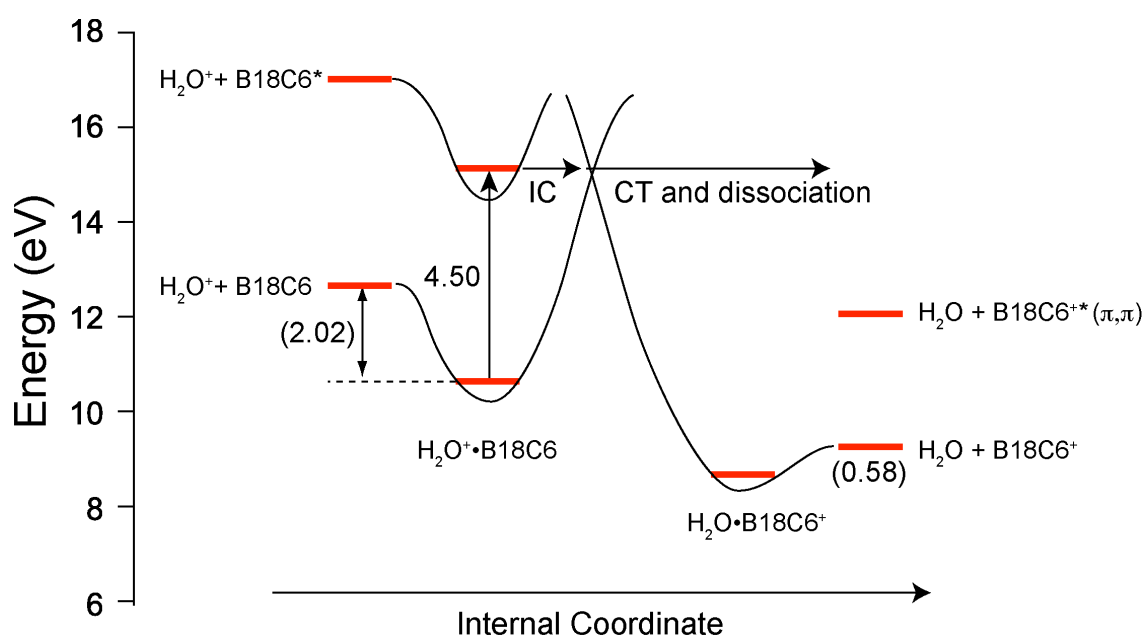


**Figure 5.** Potential energy surfaces proposed for the  $(\text{H}_2\text{O}\cdot\text{B18C6})^+$  complex. The vertical axis is the energy with respect to the energy of  $\text{H}_2\text{O} + \text{B18C6}$ .

## References

- (1) Fenn, J. B.; Mann, M.; Meng, C. K.; Wong, S. F.; Whitehouse, C. M., Electrospray Ionization for Mass-Spectrometry of Large Biomolecules. *Science* **1989**, *246*, 64-71.
- (2) Kebarle, P.; Verkerk, U. H., Electrospray: From Ions in Solution to Ions in the Gas Phase, What We Know Now. *Mass Spectrom. Rev.* **2009**, *28*, 898-917.
- (3) Blades, A. T.; Jayaweera, P.; Ikonomou, M. G.; Kebarle, P., First Studies of the Gas Phase Ion Chemistry of  $M^{3+}$  Metal Ion Ligands. *Int. J. Mass Spectrom. Ion Processes* **1990**, *101*, 325-336.
- (4) Svendsen, A.; Lorenz, U. J.; Boyarkin, O. V.; Rizzo, T. R., A New Tandem Mass Spectrometer for Photofragment Spectroscopy of Cold, Gas-Phase Molecular Ions. *Rev. Sci. Instrum.* **2010**, *81*, 073107.
- (5) Inokuchi, Y.; Boyarkin, O. V.; Kusaka, R.; Haino, T.; Ebata, T.; Rizzo, T. R., UV and IR Spectroscopic Studies of Cold Alkali Metal Ion-Crown Ether Complexes in the Gas Phase. *J. Am. Chem. Soc.* **2011**, *133*, 12256-12263.
- (6) Inokuchi, Y.; Ebata, T.; Rizzo, T. R.; Boyarkin, O. V., Microhydration Effects on the Encapsulation of Potassium Ion by Dibenzo-18-Crown-6. *J. Am. Chem. Soc.* **2014**, *136*, 1815-1824.
- (7) Boyarkin, O. V.; Mercier, S. R.; Kamariotis, A.; Rizzo, T. R., Electronic Spectroscopy of Cold, Protonated Tryptophan and Tyrosine. *J. Am. Chem. Soc.* **2006**, *128*, 2816-2817.
- (8) Rizzo, T. R.; Stearns, J. A.; Boyarkin, O. V., Spectroscopic Studies of Cold, Gas-Phase Biomolecular Ions. *Int. Rev. Phys. Chem.* **2009**, *28*, 481-515.
- (9) Nagornova, N. S.; Rizzo, T. R.; Boyarkin, O. V., Exploring the Mechanism of IR-UV Double-Resonance for Quantitative Spectroscopy of Protonated Polypeptides and Proteins. *Angew. Chem. Int. Ed.* **2013**, *52*, 6002-6005.
- (10) Inokuchi, Y.; Boyarkin, O. V.; Kusaka, R.; Haino, T.; Ebata, T.; Rizzo, T. R., Ion Selectivity of Crown Ethers Investigated by UV and IR Spectroscopy in a Cold Ion Trap. *J. Phys. Chem. A* **2012**, *116*, 4057-4068.
- (11) Kusaka, R.; Inokuchi, Y.; Ebata, T., Water-Mediated Conformer Optimization in Benzo-18-Crown-6-Ether/Water System. *Phys. Chem. Chem. Phys.* **2009**, *11*, 9132-9140.
- (12) Dinelli, B. M.; Crofton, M. W.; Oka, T., Infrared Spectroscopy of the  $\nu_3$  Band of  $H_2O^+$ . *J. Mol. Spectrosc.* **1988**, *127*, 1-11.
- (13) Shubert, V. A.; James, W. H.; Zwier, T. S., Jet-Cooled Electronic and Vibrational Spectroscopy of Crown Ethers: Benzo-15-Crown-5 Ether and 4'-Amino-Benzo-15-Crown-5 Ether. *J. Phys. Chem. A* **2009**, *113*, 8055-8066.
- (14) Shubert, V. A.; Muller, C. W.; Zwier, T. S., Water's Role in Reshaping a Macrocyclic Binding Pocket: Infrared and Ultraviolet Spectroscopy of Benzo-15-Crown-5- $(H_2O)_n$  and 4'-Aminobenzo-15-Crown-5- $(H_2O)_n$ ,  $n = 1, 2$ . *J. Phys. Chem. A* **2009**, *113*, 8067-8079.
- (15) Snow, K. B.; Thomas, T. F., Mass Spectrum, Ionization Potential, and Appearance Potentials for Fragment Ions of Sulfuric Acid Vapor. *Int. J. Mass Spectrom. Ion Processes* **1990**, *96*, 49-68.
- (16) Nemeth, G. I.; Selzle, H. L.; Schlag, E. W., Magnetic Zeke Experiments with Mass Analysis. *Chem. Phys. Lett.* **1993**, *215*, 151-155.

- (17) Frisch, M. J.; Trucks, G. W.; Schlegel, H. B.; Scuseria, G. E.; Robb, M. A.; Cheeseman, J. R.; Scalmani, G.; Barone, V.; Mennucci, B.; Petersson, G. A. *et al.*, In *Gaussian 09, Revision A.1*; Gaussian, Inc.: Wallingford CT, 2009.
- (18) Rodgers, M. T.; Armentrout, P. B., Noncovalent Metal–Ligand Bond Energies as Studied by Threshold Collision-Induced Dissociation. *Mass Spectrom. Rev.* **2000**, *19*, 215-247.
- (19) Tachikawa, H.; Takada, T., Proton Transfer Rates in Ionized Water Clusters  $(\text{H}_2\text{O})_n$  ( $n = 2-4$ ). *RSC Advances* **2015**, *5*, 6945-6953.
- (20) Ma, J.; Schmidhammer, U.; Pernot, P.; Mostafavi, M., Reactivity of the Strongest Oxidizing Species in Aqueous Solutions: The Short-Lived Radical Cation  $\text{H}_2\text{O}^{\bullet+}$ . *J. Phys. Chem. Lett.* **2014**, *5*, 258-261.
- (21) Li, J.; Nie, Z.; Zheng, Y. Y.; Dong, S.; Loh, Z.-H., Elementary Electron and Ion Dynamics in Ionized Liquid Water. *J. Phys. Chem. Lett.* **2013**, *4*, 3698-3703.
- (22) Furuhashi, A.; Dupuis, M.; Hirao, K., Reactions Associated with Ionization in Water: A Direct Ab Initio Dynamics Study of Ionization in  $(\text{H}_2\text{O})_{17}$ . *J. Chem. Phys.* **2006**, *124*, 164310.
- (23) Marsalek, O.; Elles, C. G.; Pieniasek, P. A.; Pluhařová, E.; VandeVondele, J.; Bradforth, S. E.; Jungwirth, P., Chasing Charge Localization and Chemical Reactivity Following Photoionization in Liquid Water. *J. Chem. Phys.* **2011**, *135*, 224510.
- (24) Gauduel, Y.; Pommeret, S.; Migus, A.; Antonetti, A., Some Evidence of Ultrafast  $\text{H}_2\text{O}^+$ -Water Molecule Reaction in Femtosecond Photoionization of Pure Liquid Water: Influence on Geminate Pair Recombination Dynamics. *Chem. Phys.* **1990**, *149*, 1-10.
- (25) Lide, D. R., CRC Handbook of Chemistry and Physics. 82nd Edition; CRC Press LLC: Boca Raton, London, New York, Washington, D. C., 2001.
- (26) Ohashi, K.; Nishi, N., Photodissociation Spectroscopy of Benzene Cluster Ions:  $(\text{C}_6\text{H}_6)_2^+$  and  $(\text{C}_6\text{H}_6)_3^+$ . *J. Chem. Phys.* **1991**, *95*, 4002-4009.
- (27) Ohashi, K.; Nishi, N., Photodissociation Dynamics of  $(\text{C}_6\text{H}_6)_3^+$ : Role of the Extra Benzene Molecule Weakly Bound to the Dimer Core. *J. Chem. Phys.* **1998**, *109*, 3971-3982.
- (28) Messina, F.; Bräm, O.; Cannizzo, A.; Chergui, M., Real-Time Observation of the Charge Transfer to Solvent Dynamics. *Nat. Commun.* **2013**, *4*, 2119.

TOC Figure

